

An intracavity, frequency-doubled BaWO₄ Raman laser generating multi-watt continuous-wave, yellow emission

Andrew J. Lee^{1*}, Helen M. Pask¹, James A. Piper¹, Huaijin Zhang², and Jiyang Wang²

¹MQ Photonics, Department of Physics and Engineering, Macquarie University, Sydney, NSW, 2109, Australia

²State Key Laboratory of Crystal Materials and Institute of Crystal Materials, Shandong University, Jinan, 250100, PR China

*alee@ics.mq.edu.au

Abstract: We report the generation of multi-watt continuous-wave (CW) yellow laser emission from an intracavity diode-pumped Nd:GdVO₄/BaWO₄ Raman laser utilising a high-Q resonator (for fundamental and first-Stokes wavelengths) and intracavity frequency-doubling in LBO. CW output power of 2.9 W is achieved with a high overall diode-to-yellow conversion efficiency of 11% and with good beam quality ($M^2 \sim 2.5$).

©2010 Optical Society of America

OCIS codes: (140.3550) Lasers, Raman; (190.2620) Nonlinear optics, frequency conversion; (140.3380) Lasers, diode-pumped.

References and links

1. P. Cerny, H. Jelinkova, P. G. Zverev, and T. T. Basiev, "Solid state lasers with Raman frequency conversion," *Prog. Quantum Electron.* **28**(2), 113–143 (2004).
2. T. T. Basiev, and R. C. Powell, in: *Handbook of Laser Technology and Applications*, C. E. Webb, J. D. C. Jones, eds., (Institute of Physics, UK, 2003).
3. J. A. Piper, and H. M. Pask, "Crystalline Raman lasers," *IEEE Sel. Top. Quantum. Electron.* **13**(3), 692–704 (2007).
4. H. M. Pask, P. Dekker, R. P. Mildren, D. J. Spence, and J. A. Piper, "Wavelength-versatile visible and UV sources based on crystalline Raman lasers," *Prog. Quantum Electron.* **32**(3-4), 121–158 (2008).
5. M. L. Wolbarsht and M. B. Landers III, "Some considerations for choosing the wavelength appropriate for laser photocoagulation of the retina," *Laser Treatment and Photocoagulation of the Eye, Proceedings*, 10–19, 1983.
6. A. J. Lee, H. M. Pask, P. Dekker, and J. A. Piper, "High efficiency, multi-Watt CW yellow emission from an intracavity-doubled self-Raman laser using Nd:GdVO₄," *Opt. Express* **16**(26), 21958–21963 (2008).
7. R. P. Mildren, H. M. Pask, H. Ogilvy, and J. A. Piper, "Discretely tunable, all-solid-state laser in the green, yellow, and red," *Opt. Lett.* **30**(12), 1500–1502 (2005).
8. Z. Cong, X. Zhang, Q. Wang, Z. Liu, S. Li, X. Chen, X. Zhang, S. Fan, H. Zhang, and X. Tao, "Efficient diode-end-pumped actively Q-switched Nd:YAG/SrWO₄/KTP yellow laser," *Opt. Lett.* **34**(17), 2610–2612 (2009).
9. P. Dekker, H. M. Pask, and J. A. Piper, "All-solid-state 704 mW continuous-wave yellow source based on an intracavity, frequency-doubled crystalline Raman laser," *Opt. Lett.* **32**(9), 1114–1116 (2007).
10. H. M. Pask, "Continuous-wave, all-solid-state, intracavity Raman laser," *Opt. Lett.* **30**(18), 2454–2456 (2005).
11. W. Ge, H. Zhang, J. Wang, J. Liu, H. Li, X. Cheng, H. Xu, X. Xu, X. Hu, and M. Jiang, "The thermal and optical properties of BaWO₄ single crystal," *J. Cryst. Growth* **276**(1-2), 208–214 (2005).
12. W. W. Ge, H. J. Zhang, J. Y. Wang, J. H. Liu, X. G. Xu, X. B. Hu, M. H. Jiang, D. G. Ran, S. Q. Sun, H. R. Xia, and R. I. Boughton, "Thermal and mechanical properties of BaWO₄ crystal," *J. Appl. Phys.* **98**(1), 013542–013546 (2005).
13. P. Erný and H. Jelínková, "Near-quantum-limit efficiency of picosecond stimulated Raman scattering in BaWO₄ crystal," *Opt. Lett.* **27**(5), 360–362 (2002).
14. Y. F. Chen, K. W. Su, H. J. Zhang, J. Y. Wang, and M. H. Jiang, "Efficient diode-pumped actively Q-switched Nd:YAG/BaWO₄ intracavity Raman laser," *Opt. Lett.* **30**(24), 3335–3337 (2005).
15. S. Li, X. Zhang, Q. Wang, X. Zhang, Z. Cong, H. Zhang, and J. Wang, "Diode-side-pumped intracavity frequency-doubled Nd:YAG/BaWO₄ Raman laser generating average output power of 3.14 W at 590 nm," *Opt. Lett.* **32**(20), 2951–2953 (2007).
16. L. Fan, Y.-X. Fan, Y.-Q. Li, H. Zhang, Q. Wang, J. Wang, and H.-T. Wang, "High-efficiency continuous-wave Raman conversion with a BaWO₄ Raman crystal," *Opt. Lett.* **34**(11), 1687–1689 (2009).
17. V. Lupei, N. Pavel, Y. Sato, and T. Taira, "Highly efficient 1063-nm continuous-wave laser emission in Nd:GdVO₄," *Opt. Lett.* **28**(23), 2366–2368 (2003).

18. D. J. Spence, P. Dekker, and H. M. Pask, "Modeling of continuous wave intracavity Raman lasers," *J. Sel. Top. Quantum Electron.* **13**(3), 756–763 (2007).
19. A. J. Lee, H. M. Pask, T. Omatsu, P. Dekker, and J. A. Piper, "All-solid-state continuous-wave yellow laser based on intracavity frequency-doubled self-Raman laser," *Appl. Phys. B* **88**(4), 539–544 (2007).
20. P. Dekker, H. M. Pask, D. J. Spence, and J. A. Piper, "Continuous-wave, intracavity doubled, self-Raman laser operation in Nd:GdVO₄ at 586.5 nm," *Opt. Express* **15**(11), 7038–7046 (2007).
21. A. E. Siegman, "Analysis of laser beam quality degradation caused by quartic phase aberrations," *Appl. Opt.* **32**(30), 5893–5901 (1993).
22. T. T. Basiev, A. V. Gavrilov, V. V. Osiko, S. N. Smetanin and A. V. Fedin, "High-average-power SRS conversion of radiation in a BaWO₄ crystal," *Quantum Electron.* **34**, 649–651 (2004).
23. J. L. Blows, P. Dekker, P. Wang, J. M. Dawes, and T. Omatsu, "Thermal lensing measurements and thermal conductivity of Yb:YAB," *Appl. Phys. B* **76**(3), 289–292 (2003).
24. A. S. Grabtchikov, A. N. Kuzmin, V. A. Lisinetskii, G. I. Ryabtsev, V. A. Orlovich, and A. A. Demidovich, "Stimulated Raman scattering in Nd:KGW laser with diode pumping," *J. Alloy. Comp.* **300-301**(1-2), 300–302 (2000).

1. Introduction

There have been significant advances recently in using Stimulated Raman Scattering (SRS) in crystalline Raman materials to extend the output wavelength capability of all-solid-state lasers [1–3]. The combination of Raman conversion and frequency-doubling has enabled the generation of wavelengths spanning the ultra-violet (UV) to the visible and infrared [4]. Multi-Watt continuous-wave (CW) yellow lasers have numerous applications in the biomedical and display arenas. In particular, there is growing demand for CW laser sources operating in the yellow-orange spectral region, for retinal photocoagulation, since these wavelengths are highly absorbed by haemoglobin (oxy- and deoxy-), but are removed from the absorption band of xanthophylls (the absorbing centres in the macula) [5], and therefore have less potential to cause collateral damage to eye compared with the green sources most commonly used to date.

Several of the current authors have previously reported a 2.5 W CW yellow (586 nm) laser source incorporating intracavity-frequency-doubling (in LBO) of an Nd:GdVO₄ self-Raman laser [6]. While self-Raman lasers are very attractive for miniaturisation (since they generate the fundamental and Raman fields in the one crystal) and have the additional benefit of minimising resonator losses (by removing insertion loss associated with a second crystal), they do have disadvantages in that they offer restricted wavelength options, and suffer from high heat loading (due to the combined effects of waste-pump, quantum-defect and Raman heating) which limits output power and beam quality. An approach using separate laser and Raman crystals offers both greater output wavelength flexibility and potential for greater power scaling. The output wavelength flexibility arises from the range of fundamental wavelengths and Raman shifts available from different laser and Raman laser crystals, while the power scaling potential comes from distributing the thermal load between two crystals, and for example using large mode sizes to control the thermal lens in the laser crystal. This approach has already been demonstrated for pulsed (Q-switched) diode-pumped fundamental/Raman lasers with intracavity frequency-doubling [7,8]. Our own early reports of CW Raman lasers [9,10] also used a separate Raman crystal, however the insertion loss associated with the extra crystal impacted on threshold and efficiency. Accordingly, we are now exploring a range of different Raman laser crystals in combination with different fundamental laser crystals, to extend the capability of CW visible sources based on frequency-doubled Raman lasers.

A relatively new and very promising Raman-active material for efficient, high power Raman conversion is BaWO₄. A uniaxial crystal, it features very high Raman gain (~8.5 cm/GW) [11], narrow Raman linewidth (~0.97 cm⁻¹ at 925 cm⁻¹) [11] and reasonable thermal conductivity (~2.3 Wm⁻¹K⁻¹) [12]. In early studies, Cerny *et al* demonstrated near-quantum-limit (>95%) conversion efficiency of 532 nm picosecond pulses to the first-Stokes [13]. The application of BaWO₄ for intracavity Raman-shifting of Q-switched lasers was later reported by Chen [14], who demonstrated intracavity first-Stokes shifting of an end-pumped

Nd:YAG laser (achieving 1.56 W of output at 1181 nm with a 16.9% diode to first-Stokes conversion efficiency). Li *et al* later included intra-cavity KTP in a side-pumped Nd:YAG Q-switched laser and demonstrated 3.14 W of frequency-doubled first-Stokes emission at 590 nm [15]. More recently, by using high-Q resonators for the fundamental and first-Stokes wavelengths, continuous-wave (CW) Raman conversion in a 30 mm long BaWO₄ crystal has been reported with first-Stokes output as high as 3.36 W and diode-to-Stokes conversion efficiency of 13.2% [16]; this is the highest reported conversion efficiency from a CW crystalline Raman laser. The high Raman gain of BaWO₄ is especially advantageous because in principle, it compensates for the additional insertion losses observed when using a two-crystal configuration, in comparison to a self-Raman configuration.

In this paper, we report the first demonstration of high efficiency, multi-Watt CW yellow laser emission ($\lambda = 590$ nm) from an intracavity end-pumped BaWO₄ Raman laser incorporating an intracavity lithium borate (LBO) crystal for frequency doubling of the 1180 nm first-Stokes wavelength.

2. Experimental arrangement

A 4 × 4 × 48 mm, a-cut BaWO₄ crystal, grown by the Institute of Crystal Materials, Shandong University was used for the experiments. Two resonator configurations were employed, one to investigate performance at the first-Stokes wavelength (1180 nm), and another to evaluate the frequency-doubled (yellow) performance. Details of each resonator are summarised in Table 1 and Figs. 1(a) and 1(b). In both cases the Nd:GdVO₄ fundamental laser crystal was pumped by a 30 W, 880 nm, fibre-coupled laser diode (200 μ m core diameter, 0.22 NA, LIMO). The 880 nm diode was chosen to match the ⁴I_{9/2} – ⁴F_{3/2} absorption transition in the Nd³⁺ ion. This direct pumping of the upper laser level for the 1063 nm fundamental is effective in reducing thermal loading of the Nd:GdVO₄ crystal [17]. The pump beam was focussed to a 430 μ m spot diameter (63 mrad half-angle divergence) using a two-lens system, and was incident on the 4 × 4 × 10 mm 0.3 at. % Nd:GdVO₄ laser crystal (a-cut, AR coated for 880 nm, 1063 nm and 1180 nm) through mirror M1. The BaWO₄ crystal was also anti-reflection (AR) coated for 880 nm, 1063 nm and 1180 nm; both the laser and Raman crystals were mounted in water-cooled copper blocks maintained at a temperature of 20 °C. For yellow generation, the resonator further incorporated a non-critically phase matched (NCPM) lithium borate (LBO) crystal (dimensions 4 × 4 × 10 mm with both surfaces AR coated for 1063 nm – 1180 nm). The LBO crystal was maintained at a temperature of 41.5 °C in order to frequency double the first-Stokes emission from the BaWO₄ crystal.

Details of resonator mirror curvatures and coatings are given in Table 1. The total lengths of the first-Stokes and yellow configured resonators were ~60 mm and ~73 mm respectively.

Table 1. Summary of resonator elements.

Element	Description
M1	Flat mirror: R >99.994% @ 1064 nm/1180 nm, T >96% at 808/880 nm
M2	Flat dichroic mirror: side facing the Nd:GdVO ₄ coated AR (R < 0.06%) at 1063 and 1180 nm, side facing the LBO coated AR (R < 0.06%) at 1064 and 1180 nm, and HR at 586.5 nm (R = 98.7%).
M3	Stokes Resonator: 250 mm ROC mirror, coated HR: R = 99.91% @ 1064 nm; R = 99.6% @ 1180 nm. Yellow Resonator: 300 mm ROC mirror: Coated HR: R >99.994% @ 1064 nm/1180 nm and AR 808/880 nm
Nd:GdVO ₄ crystal	Coated AR: R = 2.54% @ 880 nm; R = 0.017% @ 1063 nm; R = 0.049% @ 1180 nm
BaWO ₄ crystal	Coated AR: R = 1.25% @ 880 nm; R = 0.145% @ 1063 nm; R = 0.194% @ 1180 nm
LBO crystal	Coated AR: R = 0.785% @ 588 nm; R = 0.146% @ 1063 nm; R = 0.338% @ 1180 nm

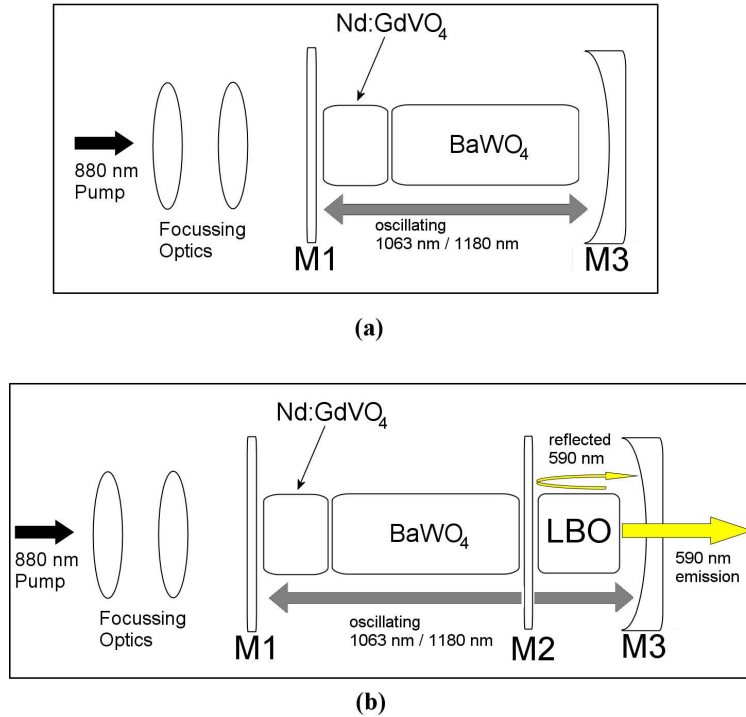


Fig. 1. Resonator layout for (a) first-Stokes generation and; (b) yellow generation.

3. Results

3.1 BaWO₄ first-Stokes power scaling performance

The first-Stokes power scaling performance is shown in Fig. 2. By rotating the Nd:GdVO₄ crystal, we could choose to polarise the fundamental ($\lambda = 1063$ nm) beam parallel to either the BaWO₄ crystal “b” or “c”-axes.

First-Stokes emission occurred at 1180 nm, consistent with SRS of the fundamental 1063 nm wavelength on the 925 cm^{-1} mode. Thresholds of 2.4 W and 2.5 W (incident diode-pump power) were obtained for fundamental polarisation parallel to the c-axis and b-axis respectively, and the first-Stokes laser performance is shown in Fig. 2. A maximum first-Stokes emission of 2.1 W was obtained for 27 W incident pump power, with the corresponding conversion efficiency (diode – 1180 nm) being 7.8%. This was obtained with the fundamental polarised parallel to the b-axis of the BaWO₄. When the fundamental polarisation was parallel to the c-axis of the BaWO₄, the output power decreased for incident pump powers above ~17 W. This decrease coincided with the onset of a secondary Raman laser line at 1102 nm, as shown in the output spectrum (see inset in Fig. 2). The laser output on this secondary Raman line was also polarised parallel to the c-axis.

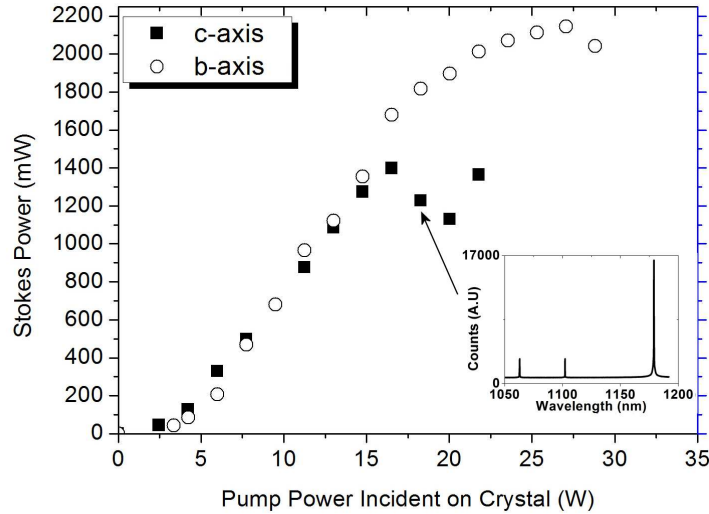


Fig. 2. First-Stokes power scaling using a 48 mm long a-cut BaWO₄ crystal.

We examined the spontaneous Raman spectra (SRS) of the BaWO₄ crystal (using a Renishaw In-Via Raman spectrometer) with incident excitation light polarised parallel to either the b or c axes. The SRS spectra were normalised to the strongest emission peak (at 925 cm⁻¹ in both cases) and these are shown in Fig. 3. The spectra show strong peaks at 925 cm⁻¹ for light polarised parallel to the two orthogonal crystal axes, with weaker modes also observed at 332 cm⁻¹ for both axes, and at 830 cm⁻¹ for polarisation parallel to the b-axis only.

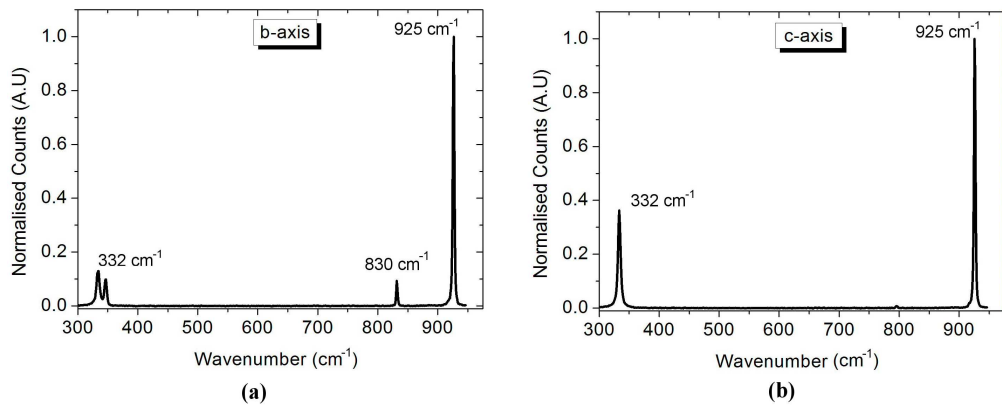


Fig. 3. Spontaneous Raman spectra for excitation polarised parallel to the (a) b-axis and; (b) c-axis of a-cut BaWO₄. Spectra are normalised to the 925 cm⁻¹ mode.

The secondary emission line at 1102 nm corresponds to a wavelength shift of 332cm⁻¹, for SRS of the fundamental polarised parallel to the c-axis. The Raman peak at 332 cm⁻¹ in the spontaneous Raman spectra of Fig. 3 was significantly stronger (by a factor of approximately 3.5 relative to the 925 cm⁻¹ peak) when the excitation light was polarised parallel to the c-axis compared to the b-axis. This is consistent with our observations of the CW Raman emission spectra where no secondary emission lines were observed when the fundamental was polarised parallel to the b-axis.

At the higher incident powers (> 25 W), and for the case of fundamental polarisation along the BaWO₄ b-axis, the output power rolled over and became increasingly sensitive to

resonator alignment. This sensitivity, which is characteristic of resonator instability, likely results from thermal loading of the Nd:GdVO₄ and BaWO₄ crystals and consequent thermal lensing. Consistent with the conclusions of Fan *et al* [16], we expect that a shorter BaWO₄ crystal (~30 mm length) may offer higher first-Stokes output due to improved resonator stability for high incident pump powers, albeit at the expense of a higher threshold.

The first-Stokes threshold and output power reported here compares well with the first-Stokes CW emission threshold of 3.7 W, and maximum output power of 2.4 W obtained using a 50 mm a-cut BaWO₄ crystal, as reported in [16]. It is interesting to note that in [16], higher first-Stokes laser output for light polarised parallel to the c-axis of the BaWO₄ crystal (c.f. b-axis) was reported but there was no mention of any secondary emission lines. Also, given the similarity in mirror transmission losses for the resonator detailed here and in [16], the lower threshold reported here (2.5 W c.f. 3.7 W) may suggest that the system in [16] had higher internal losses. We did not attempt further optimisation of the first Stokes output since the focus of this study was on the generation of yellow emission. However, it is likely that higher first Stokes output would be achieved by a combination of higher output coupling and reduction of resonator losses, which include those associated with the BaWO₄ crystal. A numerical analysis of CW Raman lasers with and without intracavity doubling can be found in [18].

3.2 BaWO₄ yellow power scaling results

The yellow resonator was setup with an output coupler having radius of curvature of 300 mm. ABCD resonator modelling showed that the laser resonator supported lowest order transverse modes with diameters which closely overlapped the pump spot within the laser crystal. Mode diameters ranging from ~330 μm to ~530 μm in the laser crystal were calculated under the assumption of both weak (200 mm effective focal length) and strong (45 mm effective focal length) thermal lenses in the laser crystal. The mode diameters in the BaWO₄ and LBO crystals were found to gradually contract (from initial values of ~346 μm and ~352 μm in the BaWO₄ and LBO crystals respectively to ~180 μm and ~150 μm) as the thermal lens increased in strength. This reduction in mode size within the BaWO₄ and LBO crystals is advantageous as it acts to increase the non-linear couplings.

The power scaling performance at 590 nm is shown in Fig. 4. The Nd:GdVO₄ crystal was oriented with the b-axis of the BaWO₄ crystal parallel to the polarisation of the laser fundamental. A maximum output power of 2.9 W at 590 nm was obtained corresponding to 11% optical conversion efficiency (diode to yellow). The output beam quality (measured using a Gentec Beamscope) varied between $M^2 \sim 1.32$ for pump powers close to threshold to $M^2 \sim 2.5$ at maximum incident pump power in a beam of near Gaussian profile.

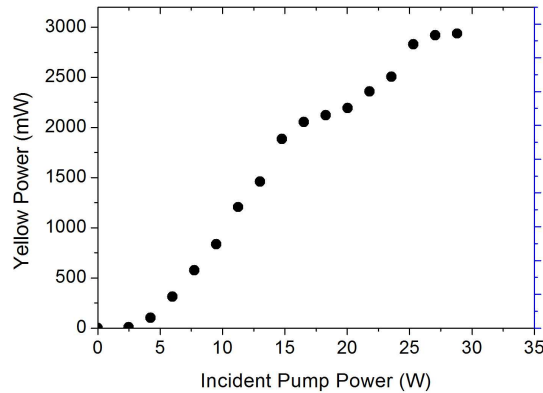


Fig. 4. Yellow power scaling performance achieved by intracavity frequency-doubling the first-Stokes emission from an a-cut BaWO₄ crystal.

The spectral content of the residual infrared output leaking from the cavity was monitored and found to include only the fundamental at 1064 nm and the first-Stokes Raman laser line at 1180 nm. No output at 1102 nm could be observed.

It is interesting to compare the relative performance of this laser with that previously reported for a frequency-doubled Nd:GdVO₄/KGW Raman laser [9], and a frequency-doubled Nd:GdVO₄ self-Raman laser [6]. The diode-pump threshold and maximum output power for yellow generation, overall diode-yellow conversion efficiency and beam quality of the three systems are summarised in Table 2. Note that in [9], pumping was at 808 nm and that there was no intracavity mirror.

Table 2. Comparison of yellow emission threshold, maximum yellow power, overall efficiency and beam quality for an Nd:GdVO₄/KGW Raman laser [9], a self-Raman Nd:GdVO₄ laser [6] and the laser reported herein.

Properties of yellow emission	Nd:GdVO ₄ /KGW [9]	Nd:GdVO ₄ self-Raman [6]	Nd:GdVO ₄ /BaWO ₄ this study
Wavelength (nm)	588	586.5	590
Threshold-Incident Pump Power (W)	~4 W	~0.7 W	2.5 W
Maximum Yellow (W)	0.7 W@18W	2.5 W@20W	2.9 W@27W
Overall Diode-to-yellow efficiency	5.1%	12.2%	11%
Beam Quality at maximum pump (M2)	~2.1 – 2.5	~6	~2.5

Table 2 shows that the overall yellow power achieved in this work is higher than that reported in [9] and [6]. Threshold for the Nd:GdVO₄/BaWO₄/LBO system was lower compared to the Nd:GdVO₄/KGW/LBO system, most likely reflecting the higher Raman gain of BaWO₄. The considerably lower threshold for the self-Raman laser highlights the lower internal losses associated with the self-Raman resonator (two crystals instead of three). It is interesting to note that the Nd:GdVO₄/KGW and Nd:GdVO₄/BaWO₄ systems exhibited significantly better beam quality in comparison with the self-Raman resonator. Previous studies of self-Raman lasers systems [6,19,20] have shown that thermal lensing within the combined laser-Raman crystal is significant (effective focal lengths of < 30 mm being reported [19,20]) and this limits power scaling of such systems. A significant portion of this heating is due to the inelastic SRS process [20]. The present system is not subject to SRS heating within the laser crystal because the SRS process takes place in the separate Raman

crystal. Consequently, the thermal loading within the (fundamental) laser crystal is lower than that observed in self-Raman lasers, and the resonator remains stable for higher incident pump powers (up to ~27 W in this work c.f. ~20 W in [6]). The higher beam quality reported here results from this reduced thermal loading within the (separate) fundamental and Raman crystals, the reduced thermal lensing in these components (particularly in the fundamental laser crystal) leading to reduced intracavity aberrations [21].

To determine whether heating of the BaWO₄ crystal affected the performance of the laser, we mounted the BaWO₄ crystal on a polytetrafluoroethylene (PTFE) block without water cooling, and we monitored its surface temperature with a thermocouple (0.1 °C resolution). When pumping at maximum incident power it was found that the temperature of the BaWO₄ peaked at ~91 °C after 3 minutes, corresponding to a heating rate of ~0.3 °C/s. By considering the change in temperature ($\Delta T = 65.4$ °C), mass (4.6 g), density (6.4×10^3 kg m⁻³) and specific heat of the crystal (300 J kg⁻¹ K⁻¹) [11,12], an estimated 0.5 W of thermal power was deposited within the crystal. The removal of active cooling of the BaWO₄ crystal did not appear to impact the yellow powers achieved from the resonator, and therefore we believe that the resultant thermal lensing within the BaWO₄ crystal was small in comparison to the thermal lens generated within the Nd:GdVO₄ crystal. Thermal lenses generated in BaWO₄ by Raman heating have previously been reported as being weak [22]. We were unable to use our estimate of thermal load in the BaWO₄ crystal to calculate the corresponding thermal lens focal length, because we were unable to find a published value for the thermo-optic coefficient in BaWO₄. Knowledge of the thermal lens focal lengths in both the laser and Raman crystals would be a great asset in the future optimisation of this laser system, and in the future we will address this by attempting to measure it interferometrically, after [23].

We estimate that the energy deficit between the fundamental and Stokes photons (~9%) contributes approximately half the thermal power deposited in the BaWO₄ crystal. It follows that a significant contribution to heating within the BaWO₄ crystal must be due to other processes (see also [19]). We have observed blue fluorescence within the BaWO₄ crystal when Stokes-shifting (see Fig. 5), a phenomenon which has previously been noted for a number of crystalline Raman lasers and is indicative of additional energy deposition within the Raman crystal. This fluorescence has been attributed by Grabtchikov *et al* to upconversion within the Nd ions [24] for the case of Nd:KGW; while this may be a possible pathway in self-Raman lasers where an Nd-doped medium also performs Stokes-shifting, the blue fluorescence has also been reported for Stokes shifting in un-doped Raman materials such as KGW [10] and BaWO₄ as noted by Fan *et al* [16] and ourselves. We have previously suggested that the blue fluorescence in the Raman crystal may be due to trace impurity absorption (by Tm³⁺) [6]. We examined the BaWO₄ and Nd:GdVO₄ crystals using inductively coupled plasma-mass spectroscopy (ICPMS) and found that while Nd:GdVO₄ shows trace levels of Tm³⁺ (0.5 ppm), the level of Tm³⁺ in the BaWO₄ is below the detectable limit (<0.005 ppm). We note that in the experiments performed here, very strong blue fluorescence was observed in the BaWO₄ Raman crystal, and negligible fluorescence was observed in the Nd:GdVO₄ crystal. Given that both crystals experience the same intracavity fundamental and first-Stokes powers, and that the Tm³⁺ levels are higher in the Nd:GdVO₄, we deduce that the fluorescence must result from a process directly associated with Raman conversion itself rather than linear or nonlinear absorption of the Stokes radiation by Tm³⁺ impurities. A further supporting observation is that the same Nd:GdVO₄ crystal exhibits strong blue fluorescence when used in a self-Raman configuration. We will conduct a more comprehensive study, including analysis of trace impurities and phonon-assisted transitions within the crystals to identify the mechanisms causing this fluorescence.

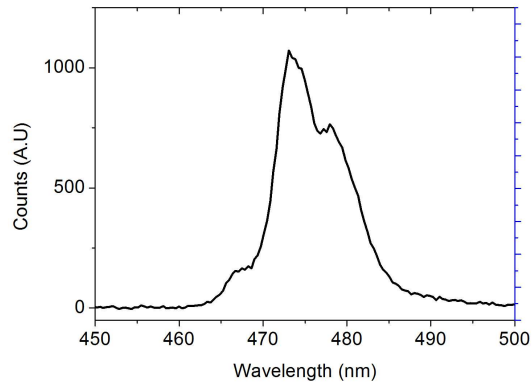


Fig. 5. Fluorescence spectrum showing blue emission observed when Stokes-shifting in BaWO₄.

4. Conclusion

We have reported the first demonstration of continuous-wave yellow emission from an intracavity frequency-doubled Nd:GdVO₄/BaWO₄ Raman laser. We have reported high first-Stokes conversion efficiency, with ~2.1 W output at 1180 nm being achieved. With the inclusion of an intracavity LBO crystal, we demonstrate high yellow emission of 2.9 W with 11% overall diode to yellow conversion efficiency at 590 nm. The output beam quality ($M^2 \sim 2.5$) was excellent and significantly better than that reported for high-power self-Raman laser systems.

Acknowledgements

This work is supported by the Commonwealth of Australia under the *International Science Linkages program*, the National Natural Science Foundation of China (No.50911120021, 50590401, 50721002), and the Grant for State Key Program of China (2010CB630702).